CHIRAL SPIN SYMMETRY AND HOT QCD*

L.Ya. Glozman

Institute of Physics, University of Graz, 8010 Graz, Austria

Received 4 March 2024, accepted 16 April 2024, published online 15 October 2024

In this paper, we overview main results indicating the existence in QCD of three qualitatively different regimes connected by smooth crossovers upon heating: a hadron gas, a stringy fluid, and a quark–gluon plasma. In the combined large-N_c and chiral limit, these regimes likely become distinct phases separated by phase transitions: a chiral restoration phase transition around $T_{\rm ch} \sim 130$ MeV and a deconfinement phase transition around $T_{\rm d} \sim 300$ MeV. It should be an important task to verify this issue on the lattice. We will introduce a chiral spin symmetry, which is a symmetry of the electric part of electrodynamics and of QCD with light quarks. It is realized approximately in QCD above the chiral restoration crossover and disappears in the QGP regime. The center symmetry of the pure glue action and the chiral spin symmetry of the electric part of the QCD Lagrangian with light quarks are complementary to distinguish the confining regime and its disappearance. We also address other lattice evidence for the stringy fluid: hadron resonances extracted from the lattice correlators; a breakdown of the thermal perturbation theory at $T < 600$ MeV and fluctuations of conserved charges that point out the N_c scaling above $T \sim 155$ MeV.

DOI:10.5506/APhysPolBSupp.17.6-A6

1. Chiral spin symmetry

Consider Maxwell equations that describe evolution of the electric and magnetic fields in a given reference frame

$$\begin{aligned} {\rm div}\vec{E} &= 4\pi\rho\,, \\ {\rm rot}\vec{B} - \frac{1}{c}\frac{\partial\vec{E}}{\partial t} &= \frac{4\pi}{c}\vec{j}\,, \\ {\rm rot}\vec{E} + \frac{1}{c}\frac{\partial\vec{B}}{\partial t} &= 0\,, \\ {\rm div}\vec{B} &= 0\,. \end{aligned} \tag{1}$$

* Presented at *Excited QCD 2024*, Benasque, Huesca, Spain, 14–20 January, 2024.

We define $\vec{E}$ and $\vec{B}$ in a given Lorentz frame in a gauge-invariant way through their action on charge and current

$$\vec{F} = q\vec{E} + q\frac{\vec{v}}{c} \times \vec{B}\,. \tag{2}$$

It is possible to measure directly $\vec{F}$ in electrodynamics but not possible in quantum chromodynamics. Is there another method to distinguish $\vec{E}$ and $\vec{B}$?

Consider charges to be massless particles with $s = 1/2$. They can be either right- or left-handed

$$\begin{pmatrix} R \\ L \end{pmatrix}. \tag{3}$$

Consider a $\mathrm{SU(2)_{CS}}$ chiral spin transformation that mixes R and L

$$\begin{pmatrix} R \\ L \end{pmatrix} \to \begin{pmatrix} R' \\ L' \end{pmatrix} = \exp\left(i\frac{\varepsilon^n \sigma^n}{2}\right) \begin{pmatrix} R \\ L \end{pmatrix}. \tag{4}$$

What happens with the charge density ρ?

$$R'^{\dagger}R' + L'^{\dagger}L' = R^{\dagger}R + L^{\dagger}L\,, \tag{5}$$

i.e.

$$\rho' = \rho\,. \tag{6}$$

The charge density is invariant under the chiral spin transformation. However, upon the chiral spin transformation, the current density $\vec{j}$ and $\vec{v}$ change. We conclude that the interaction of a charge with the electric field is invariant under the chiral spin transformation, while the interaction of a current with the magnetic field is not. This means that the chiral spin symmetry allows one to distinguish the electric and magnetic fields in a given reference frame. The electric part of the EM theory is more symmetric than the magnetic part.

The chromoelectric field of QCD is defined via the interaction with the color charge

$$\vec{F} = Q^a \vec{E}^a\,; \qquad Q^a = \int \mathrm{d}^3x\; q^{\dagger}(x) T^a q(x)\,, \qquad a = 1, \ldots, 8\,. \tag{7}$$

The color charge, which is Lorentz-invariant, is invariant under $\mathrm{SU(2)_{CS}}$

$$q \to q' = \exp\left(i\frac{\varepsilon^n \Sigma^n}{2}\right) q\,, \qquad \Sigma = \{\gamma_k, -i\gamma_5\gamma_k, \gamma_5\}\,. \tag{8}$$

In a given Lorentz frame, the interaction of quarks with the electric part of the gluonic field is chiral spin invariant like in electrodynamics. The $\mathrm{SU(2)_{CS}}$ symmetry includes $\mathrm{U(1)_A}$ as a subgroup.

We can extend the $\mathrm{SU}(2)_{\mathrm{CS}}$ symmetry to $\mathrm{SU}(2N_{\mathrm{F}})$: $\mathrm{SU}(2)_{\mathrm{CS}} \times \mathrm{SU}(N_{\mathrm{F}}) \subset \mathrm{SU}(2N_{\mathrm{F}})$ and $\mathrm{SU}(N_{\mathrm{F}})_{\mathrm{R}} \times \mathrm{SU}(N_{\mathrm{F}})_{\mathrm{L}} \times \mathrm{U}(1)_{\mathrm{A}} \subset \mathrm{SU}(2N_{\mathrm{F}})$. The $\mathrm{SU}(2N_{\mathrm{F}})$ is also a symmetry of the color charge and of the electric part of the QCD Lagrangian. *I.e.*, the color charge and electric part of the theory have an $\mathrm{SU}(2N_{\mathrm{F}})$ symmetry that is larger than the chiral symmetry of QCD as a whole. The fundamental vector of $\mathrm{SU}(2N_{\mathrm{F}})$ at $N_{\mathrm{F}} = 2$ is

$$\Psi^T = (u_{\mathrm{R}}\ u_{\mathrm{L}}\ d_{\mathrm{R}}\ d_{\mathrm{L}})\,. \tag{9}$$

Notice that the Dirac Lagrangian is not invariant under $\mathrm{SU}(2)_{\mathrm{CS}}$ and $\mathrm{SU}(2N_{\mathrm{F}})$ above — The chiral spin symmetry and its flavor extension are explicitly broken by magnetic interactions and by the quark kinetic terms.

Since the confining interaction in QCD is associated with the emergence of the color-electric flux tubes that connect static quarks, we can consider the chiral spin symmetry as a symmetry of the confining interaction with the ultrarelativistic light quarks. The necessary and sufficient conditions for the emergence of the approximate chiral spin symmetry are: *(i)* both chiral symmetries in QCD must be at least approximately restored and *(ii)* the quark-electric interaction must strongly dominate over the quark-magnetic interaction and over quark kinetic terms. The latter condition means that the physics must be dominated by a confining electric field.

The discussed symmetries were introduced in Refs. [1, 2]. For review on symmetries and their implications for hadrons and for hot QCD, see Ref. [3].

2. Emergence of the chiral spin symmetry above chiral restoration crossover and its implications

The most detailed information about QCD is encoded in correlation functions

$$C_\Gamma(t,x,y,z) = \left\langle O_\Gamma(t,x,y,z)\, O_\Gamma(0,\mathbf{0})^\dagger \right\rangle\,. \tag{10}$$

They carry the full spectral information.

In Fig. 1, we show spatial correlators of all possible $J = 0, 1$ isovector bilinears O_Γ at different temperatures obtained within $N_{\mathrm{F}} = 2$ QCD with the chirally symmetric Dirac operator [4]. We see a distinct multiplet structure of the correlators. The multiplet E1 evidences restored $\mathrm{U}(1)_{\mathrm{A}}$ symmetry (at least approximately); the multiplet E2 demonstrates approximate chiral spin and SU(4) symmetries; the multiplet E3 is consistent with chiral symmetry alone and with chiral spin (and SU(4)) symmetry and hence could be ignored. The chiral spin symmetry and its flavor extension persist up to $T \sim 500$ MeV. At larger temperatures, two distinct multiplets E1 and E2 disappear because the QCD correlators approach correlators obtained with free quarks. Notice that the latter correlators do not have the chiral spin symmetry because the Dirac Lagrangian is not CS-symmetric; for analytic

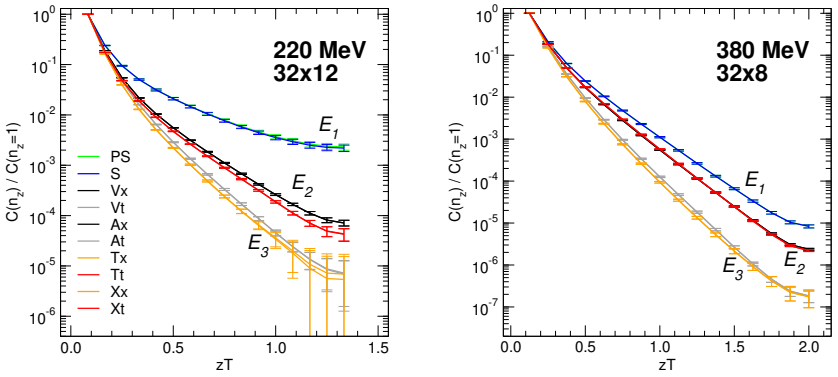

Fig. 1. Spatial correlators of all possible $J = 0, 1$ bilinears. Source: From Ref. [4].

and lattice results for all possible "free correlators", see Ref. [4]. An apparent emergence of the E1 and E2 multiplets at very high temperatures is due to the fact that at $T \to \infty$ all $J = 0, 1$ screening masses from E1 and E2 approach their limiting value $2\pi T$, which is not related to any dynamical symmetry.

In Fig. 2, we show temporal correlators for all possible $J = 0, 1$ isovector bilinears [5]. The full QCD correlators demonstrate $\mathrm{U(1)_A}$ and $\mathrm{SU(2)_L} \times \mathrm{SU(2)_R}$ multiplets as well as approximate $\mathrm{SU(2)_{CS}}$ and SU(4) multiplets. In contrast, qualitatively different correlators obtained with noninteracting quarks exhibit only $\mathrm{U(1)_A}$ and $\mathrm{SU(2)_L} \times \mathrm{SU(2)_R}$ multiplets.

We conclude that above the chiral restoration crossover, the QCD partition function is not only chiral symmetric, but is also approximately $\mathrm{SU(2)_{CS}}$ and SU(4) symmetric. This suggests that QCD is still in the confining regime until roughly 500 MeV where the confining chromoelectric field gets screened and $\mathrm{SU(2)_{CS}}$ and SU(4) symmetries smoothly disappear. Similar results have recently been obtained in $2 + 1 + 1$ QCD [6].

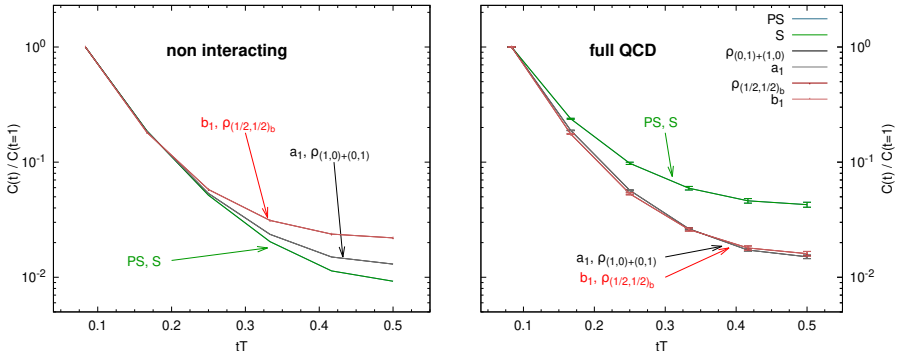

Fig. 2. Temporal correlators for 12×48^3 lattices. Left: Correlators obtained with free quarks. Right: Full QCD correlators at $T = 220$ MeV. Source: From Ref. [5].

3. Breakdown of thermal perturbation theory below 500–600 MeV

Lattice results for pseudoscalar and vector screening masses obtained at very large temperatures $T \sim$ 1–160 GeV [7] are shown in Fig. 3, left panel. They can be parameterized [7] over two orders of magnitude by

$$\begin{aligned} \frac{m_{\rm PS}}{2\pi T} &= 1 + p_2\,\hat{g}^2(T) + p_3\,\hat{g}^3(T) + p_4\,\hat{g}^4(T)\,, \\ \frac{m_{\rm V}}{2\pi T} &= \frac{m_{\rm PS}}{2\pi T} + s_4\,\hat{g}^4(T)\,, \end{aligned}$$

where p_2 is fixed by EQCD calculations and p_3, p_4, s_4 are numbers that are fitted to lattice results. A perturbative description of screening masses suggests partonic degrees of freedom, which is a signal of QGP.

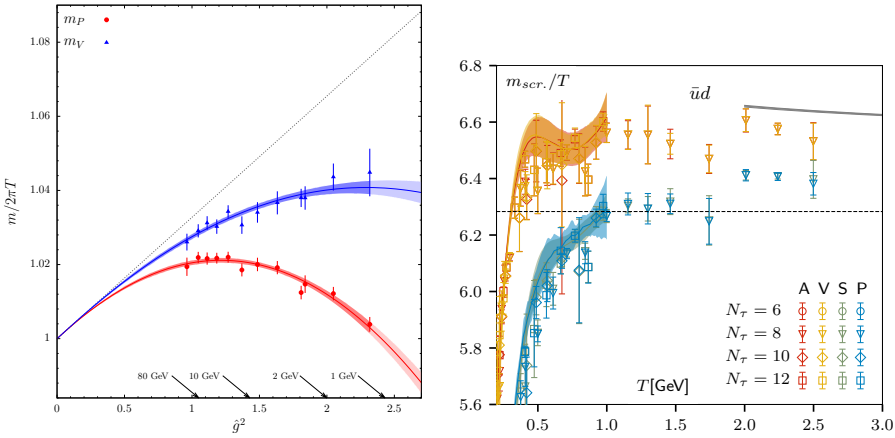

Fig. 3. Left: Temperature dependence of the pseudoscalar and vector screening masses at very large T. Source: From Ref. [7]. Right: The same but for lower temperatures. Source: From Ref. [8].

Screening masses at lower temperatures above chiral restoration crossover up to $T \sim 2.5$ GeV are shown in Fig. 3 (right) [8]. While the temperature dependence of screening masses above 500–600 MeV is flat and consistent with those shown in the left panel, at lower temperatures, the screening masses demonstrate a steep increase. The temperature dependence in the partonic (QGP) regime is only in coupling constants. Given that the coefficients p_2, p_3, p_4, s_4 are fixed by the high-T behavior of screening masses, the perturbative expansion cannot explain screening masses below 500–600 MeV. We observe an apparent change of dynamics at temperatures below 500–600 MeV. The behavior of meson screening masses from 12 different channels provides an independent demonstration of the existence of the regime below 500–600 MeV where chiral symmetry is restored but the dynamics

is inconsistent with the partonic description. The discussed behavior of screening masses must be reflected in the equation of state. Indeed, a very steep increase of p/T^4 with temperature in the same temperature interval is observed [9]. The analysis presented in this section was done in Ref. [10].

4. Pion spectral function

Direct evidence of the hadron-like degrees of freedom in the stringy fluid should be the observation of states in spectral functions. Using a finite T generalization of the Källen–Lehmann spectral representation [11], Refs. [12, 13] reconstructed pion and kaon spectral functions from the spatial lattice correlators above chiral restoration. The pion spectral function is shown in Fig. 4 [12]. The spectral function demonstrates two distinct peaks corresponding to pion and its first radial excitations. These peaks get broader with temperature and eventually melt above 500–600 MeV out. The so obtained spectral function can be controlled because it predicts the temporal correlators that can be compared with lattice results. The comparison shows good agreement at large Euclidean times.

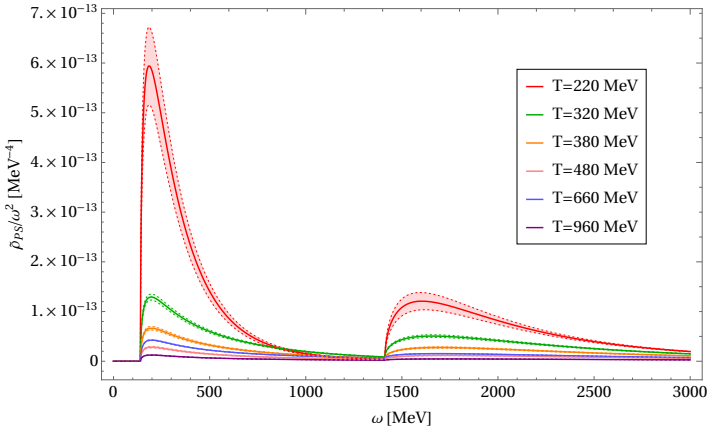

Fig. 4. Pion spectral function at different temperatures reconstructed from spatial lattice correlators presented in Fig. 1. Source: From Ref. [12].

5. Conserved charges and their fluctuations in hadron gas and at higher temperatures. Temperature evolution of the Polyakov loop

The hadron resonance gas model assumes a dilute system of point-like structureless hadrons that do not interact. For $T < 155$ MeV, the hadron resonance gas model reproduces fluctuations of conserved charges calculated on the lattice, see *e.g.* [14]. At larger temperatures, the lattice results radically deviate from the HRG model predictions.

In Ref. [15], we focus on charges associated with the net number of up, down, and strange quarks

$$N_q \equiv \int \mathrm{d}^3x \; n_q(x) \quad \text{with} \quad n_q(x) = \bar{q}(x)\gamma^0 q(x)\,, \qquad q = u, d, s\,. \tag{11}$$

Each quark can be in one of the N_c color states. This means that the conserved flavor charges N_q, scale as N_c^1. The key point is that the fluctuations of quark number densities scale as N_c^1 above chiral crossover and that in the stringy fluid phase at large N_c, they would be expected to differ from their vacuum and hadron gas values (of the order of N_c^0) by N_c.

In Fig. 5 we show typical results for fluctuations of quark numbers of u, d quarks taken from Ref. [14] and their comparison with the hadron resonance gas model. We see that the fluctuations of the quark numbers deviate from the HRG just at the chiral restoration temperature 155 MeV.

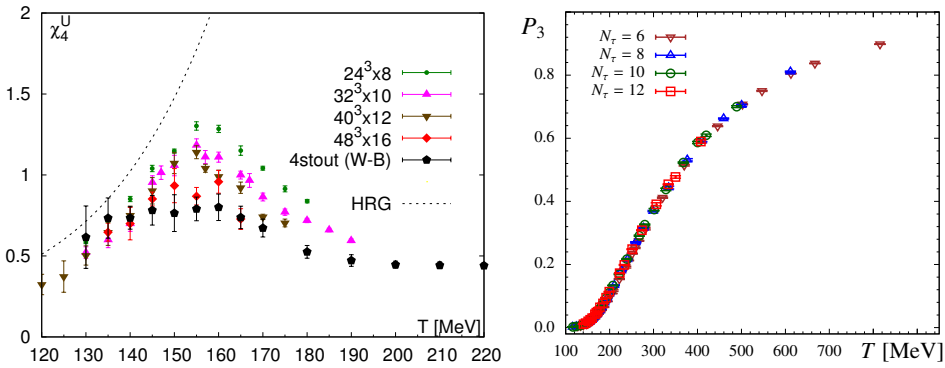

Fig. 5. Left: Fluctuations of conserved net u, d quark numbers in $2+1$ QCD at physical quark masses. Source: From Ref. [14]. Right: Temperature evolution of the properly renormalized Polyakov loop in $2+1$ QCD at physical quark masses. Source: From Ref. [19].

Since the quark numbers scale as N_c^1, the above behavior of fluctuations of conserved charges is consistent with the crossover from the hadron gas to the stringy fluid regime, where all main thermodynamical quantities scale as N_c^1 (it will be discussed in the next section). To demonstrate a transition to the QGP regime, one needs an observable that is sensitive to presence of $\sim N_c^2$ deconfined gluons. A natural observable of this kind is the Polyakov loop.

The expectation value of the Polyakov loop in a pure glue theory is the order parameter for $\mathcal{Z}_{N_c}$ center symmetry and for confinement. In the center symmetric confining phase, the expectation value of the Polyakov loop identically vanishes, while above the first-order deconfinement phase

transition at $T_{\rm d} \sim 270$–300 MeV, the center symmetry gets spontaneously broken and the expectation value of the Polyakov loop jumps to 0.5–0.6. An important issue is that the Polyakov loop in the deconfined phase, where it is not zero, is explicitly sensitive to $N_c^2 - 1$ gluons. Confining properties of QCD with light quarks and pure Yang–Mills theory are identical in the large-N_c limit. Then one expects a similar deconfinement temperature in QCD with light quarks at large N_c.

In the real world, $N_c = 3$ in QCD with light quarks, the center symmetry of the action is explicitly broken by quark loops, and the deconfinement first-order phase transition is replaced by a very smooth crossover. The renormalized Polyakov loop informs us about the deconfinement crossover region. The temperature evolution of the properly renormalized Polyakov loop, taken from Ref. [19], is shown in Fig. 5. We observe that indeed the deconfinement crossover is nothing else but a smeared broad transition around $T_{\rm d} \sim 300$ MeV. Above the chiral restoration temperature around $T_{\rm ch} \sim 155$ MeV, the Polyakov loop is very small which suggests that here QCD is in the confining regime. At the same time, at these temperatures fluctuations of conserved charges demonstrate that the hadron gas picture does not work. Both these facts are consistent with the crossover from the hadron gas to the stringy fluid. The Polyakov loop reaches the value around 0.5 at a temperature of roughly 400–500 MeV, in agreement with the temperature of smooth disappearance of the chiral spin symmetry.

6. Large N_c QCD phase diagram at $\mu_B = 0$

In previous sections, we have demonstrated numerous lattice evidence that upon increasing temperature, there are three qualitatively different regimes in QCD that are connected by smooth crossovers: a hadron gas below $T \sim 155$ MeV, an intermediate stringy fluid regime at $155 < T \lesssim 500$ MeV, and a quark–gluon plasma at higher temperatures. These regimes reflect different approximate symmetries and effective degrees of freedom. In the hadron gas, the degrees of freedom are well-separated hadrons and chiral symmetry is spontaneously broken. In the stringy fluid, chiral symmetry is restored and approximate chiral spin symmetry emerges, which is a symmetry of confining interaction. One could view this medium as a densely packed system of color-singlet clusters. The quark interchanges between clusters required by the Pauli principle should be significant. Still, it is a system with confinement. The QGP matter at high temperatures consists of deconfined quark and gluon quasiparticles.

The large-N_c limit of QCD with massless quarks should clarify issues since in this case, QCD with light quarks is manifestly center symmetric. This allows one to define unambiguously possible phases with confinement or deconfinement and with spontaneously broken or restored chiral symmetry.

Standard large-N_c analysis [16] suggests that three regimes at $N_c = 3$ and small but nonzero quark masses might become distinct phases separated by phase transitions with different scaling of main thermodynamical quantities: energy density ϵ, pressure P, and entropy density s

$$\epsilon_{\rm HG} \sim N_c^0\,, \qquad P_{\rm HG} \sim N_c^0\,, \qquad s_{\rm HG} \sim N_c^0\,, \tag{12}$$

$$\epsilon_{\rm str} \sim N_c^1\,, \qquad P_{\rm str} \sim N_c^1\,, \qquad s_{\rm str} \sim N_c^1\,, \tag{13}$$

$$\epsilon_{\rm QGP} \sim N_c^2\,, \qquad P_{\rm QGP} \sim N_c^2\,, \qquad s_{\rm QGP} \sim N_c^2\,. \tag{14}$$

A peculiar feature of the intermediate phase is that it should contain a gas of noninteracting glueballs, as in the hadron gas, while the degrees of freedom containing quarks are radically changed. Lattice large-N_c studies could clarify this picture.

It is known that the deconfinement temperature in the pure Yang–Mills theory is practically N_c-independent [17]. At the same time, confining properties of QCD with light quarks are identical to those in Yang–Mills at infinite N_c. Then one expects a deconfinement temperature in large-N_c QCD with light quarks to be around $T_{\rm d} \sim 300$ MeV. It is also found on the lattice that at $T = 0$, the quark condensate scales practically exactly as N_c^1 and the $1/N_c$ corrections are negligibly small [18]. This strongly suggests that the physics of chiral symmetry breaking in QCD at $N_c = 3$ and at large N_c is the same. Then one expects a chiral restoration phase transition in large-N_c QCD around the same temperature as at $N_c = 3$. The latter temperature was established to be around $T_{\rm ch} \sim 130$ MeV [20]. If correct, one anticipates two different phase transitions at large N_c, as was discussed above.

7. Outlook

The next important step to clarify the QCD phase diagram would be to perform lattice measurements of the chiral restoration temperature at large N_c. It is important to stress that the chiral and large-N_c limits do not commute and a proper sequence of limits should be taken. First, the large-N_c limit and then the chiral limit. This sequence of limits significantly simplifies the numerical problem. As the first step, the pure glue (quenched) configurations should be generated at large N_c. There are two strategies of doing this. The first strategy would be to employ gluonic ensembles at large volumes at reasonably large $N_c \sim$ 10–20 as was done in Ref. [17]. Then the eigenvalue problem for the Dirac operator should be solved to determine the quark condensate via the Banks–Casher relation. Upon increasing temperature, the temperature of the chiral restoration phase transition could be obtained. The alternative strategy would be to follow the Eguchi–Kawai

volume independence to address the problem at very large N_c but in a not large volume, as was done in Ref. [18]. The results for chiral restoration temperatures should give in principle the same answer in both approaches.

REFERENCES

[1] L.Ya. Glozman, *Eur. Phys. J. A* **51**, 27 (2015), arXiv:1407.2798 [hep-ph].

[2] L.Ya. Glozman, M. Pak, *Phys. Rev. D* **92**, 016001 (2015), arXiv:1504.02323 [hep-lat].

[3] L.Ya. Glozman, *Prog. Part. Nucl. Phys.* **131**, 104049 (2023), arXiv:2209.10235 [hep-lat].

[4] C. Rohrhofer *et al.*, *Phys. Rev. D* **100**, 014502 (2019), arXiv:1902.03191 [hep-lat].

[5] C. Rohrhofer, Y. Aoki, L.Ya. Glozman, S. Hashimoto, *Phys. Lett. B* **802**, 135245 (2020), arXiv:1909.00927 [hep-lat].

[6] T.W. Chiu, *Phys. Rev. D* **107**, 114501 (2023), arXiv:2302.06073 [hep-lat].

[7] M. Dalla Brida *et al.*, *J. High Energy Phys.* **2022**, 034 (2022), arXiv:2112.05427 [hep-lat].

[8] A. Bazavov *et al.*, *Phys. Rev. D* **100**, 094510 (2019), arXiv:1908.09552 [hep-lat].

[9] A. Bazavov, P. Petreczky, J.H. Weber, *Phys. Rev. D* **97**, 014510 (2018), arXiv:1710.05024 [hep-lat].

[10] L.Ya. Glozman, O. Philipsen, R.D. Pisarski, *Eur. Phys. J. A* **58**, 247 (2022), arXiv:2204.05083 [hep-ph].

[11] J. Bros, D. Buchholz, *Z. Phys. C* **55**, 509 (1992).

[12] P. Lowdon, O. Philipsen, *J. High. Energy Phys.* **2022**, 161 (2022), arXiv:2207.14718 [hep-lat].

[13] D. Bala *et al.*, arXiv:2310.13476 [hep-lat].

[14] R. Bellwied *et al.*, *Phys. Rev. D* **92**, 114505 (2015), arXiv:1507.04627 [hep-lat].

[15] T.D. Cohen, L.Ya. Glozman, arXiv:2401.04194 [hep-ph].

[16] T.D. Cohen, L.Ya. Glozman, arXiv:2311.07333 [hep-ph].

[17] B. Lucini, M. Panero, *Phys. Rep.* **526**, 93 (2013), arXiv:1210.4997 [hep-th].

[18] C. Bonanno *et al.*, arXiv:2309.15540 [hep-lat].

[19] P. Petreczky, H.P. Schadler, *Phys. Rev. D* **92**, (0945172015), arXiv:1509.07874 [hep-lat].

[20] HotQCD (H.T. Ding *et al.*), *Phys. Rev. Lett.* **123**, 062002 (2019), arXiv:1903.04801 [hep-lat].